Supplementary Information to the article "Influence of iron content on water uptake and charge transport in $BaCe_{0.6}Zr_{0.2}Y_{0.2-x}Fe_xO_{3-\delta}$ triple-conducting oxides"

Jagoda Budnik,*[a] Aleksandra Mielewczyk-Gryń,[a] Maria Gazda [a] and Tadeusz Miruszewski [a]

[a] Institute of Nanotechnology and Materials Engineering and Advanced Materials Centre, Gdańsk University of Technology, Narutowicza 11/12, 80-233, Gdańsk, Poland.
*Jagoda.budnik@pg.edu.pl

1. Additional details of Rietveld refinement

To check if other space group structures would better reflect the real symmetry of the synthesized $BaCe_{0.6}Zr_{0.2}Y_{0.2-x}Fe_xO_{3-\delta}$ compounds, the crystal data of lower symmetry perovskite structures (orthorhombic and trigonal) were used for the Rietveld refinement of collected XRD patterns. The refinement parameters obtained using cubic ($Pm\bar{3}m$), orthorhombic ($Imma$), and trigonal ($R\bar{3}c$) crystal data are summarized in **Table S1**. The XRD diffraction patterns with the corresponding fitting and differential curves are shown in **Fig. S1**. The low-intensity reflections, that should be present in the orthorhombic and trigonal patterns, were partly hidden in the noise. Nevertheless, the existence of some small distortions cannot be excluded based on these results, hence the structure of the studied materials is described as "pseudo-cubic" in the text.

Table S1. Refined structural parameters of cubic, orthorhombic, and trigonal $BaCe_{0.6}Zr_{0.2}Y_{0.2-x}Fe_xO_{3-\delta}$ (x = 0.02, 0.05, 0.1) unit cells, with used profile function, as well as the refinement quality indices (expected residual, profile residual, weighted profile residual, goodness of fit).

Parameter		BCZYFe2			BCZYFe5			BCZYFe10		
		Cubic	Orthorhombic	Trigonal	Cubic	Orthorhombic	Trigonal	Cubic	Orthorhombic	Trigonal
Unit cell	a (Å)	4.3515(1)	6.1493(4)	6.1471(2)	4.3307(1)	6.1158(2)	6.1200(2)	4.3205(2)	6.0980(4)	6.1026(2)
	b (Å)		8.6849(6)			8.6508(3)			8.6321(7)	
	c (Å)		6.1743(3)	15.1259(7)		6.1437(2)	15.0348(5)		6.1294(3)	15.0101(7)
	α (°)	90	90	90	90	90	90	90	90	90
	β (°)									
	γ (°)			120			120			120
Profile function		Pseudo Voigt								
Agreement indices	R_{exp}	4.26	4.26	4.25	5.55	5.54	5.54	12.82	12.82	12.82
	R_p	4.03	4.18	4.10	4.44	4.29	4.38	13.85	15.53	16.28
	R_{wp}	5.85	6.20	6.15	6.56	6.32	6.55	18.38	20.00	20.40
	GOF	1.89	2.12	2.09	1.40	1.30	1.39	2.06	2.44	2.53

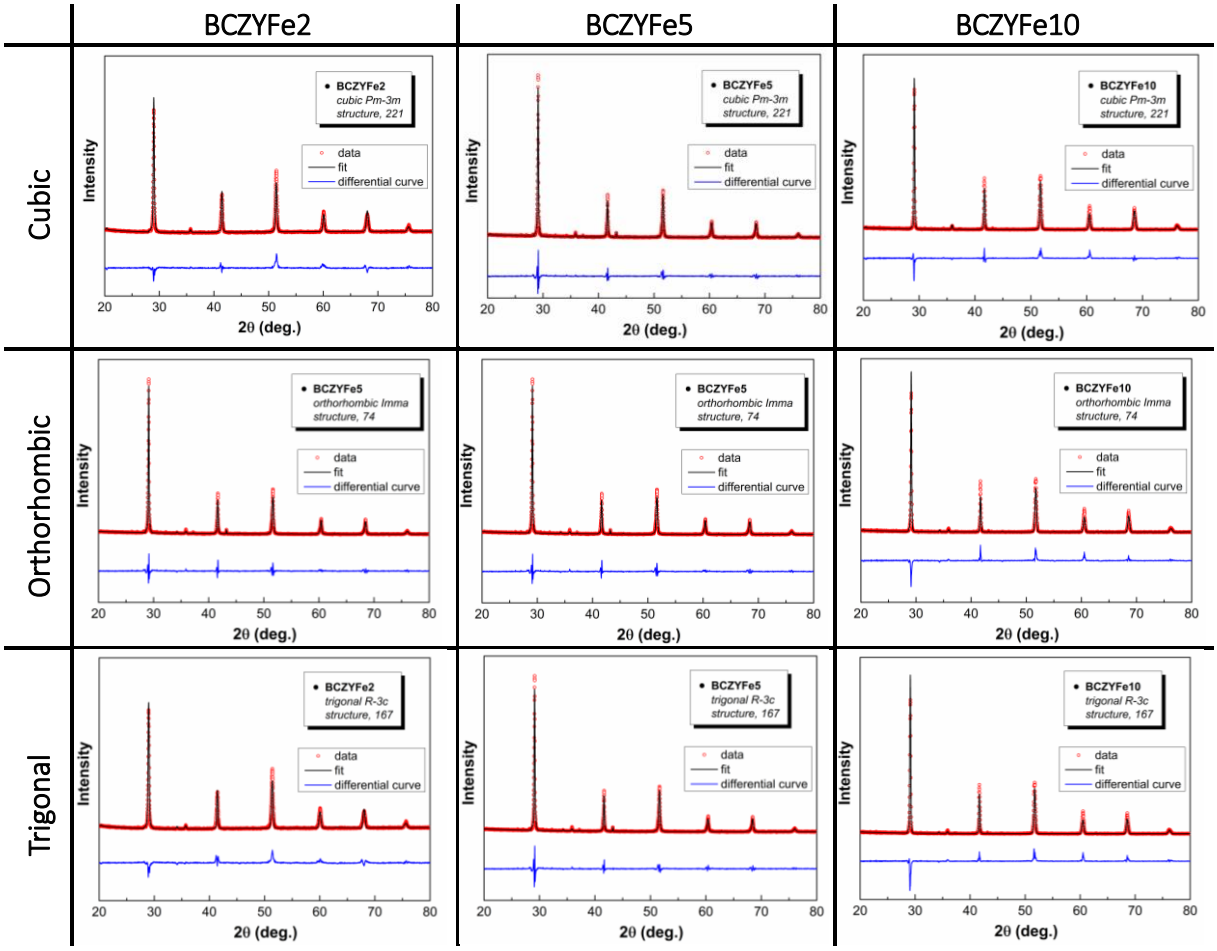

Fig. S1. XRD diffraction patterns with the corresponding fitting and differential curves for $BaCe_{0.6}Zr_{0.2}Y_{0.18}Fe_{0.02}O_{3-\delta}$ (BCZYFe2), $BaCe_{0.6}Zr_{0.2}Y_{0.15}Fe_{0.05}O_{3-\delta}$ (BCZYFe5), and $BaCe_{0.6}Zr_{0.2}Y_{0.1}Fe_{0.1}O_{3-\delta}$ (BCZYFe10), refined using cubic, orthorhombic and trigonal unit cells.

2. Additional thermogravimetric studies

Additional hydration analysis via thermogravimetry was conducted. **Fig. S2** shows the relative mass change of $BaCe_{0.6}Zr_{0.2}Y_{0.2-x}Fe_xO_{3-\delta}$ (x = 0.02, 0.05, 0.1) samples collected at 300, 450, and 600 ℃ during the atmosphere switches: from dry to wet and from wet to dry air.

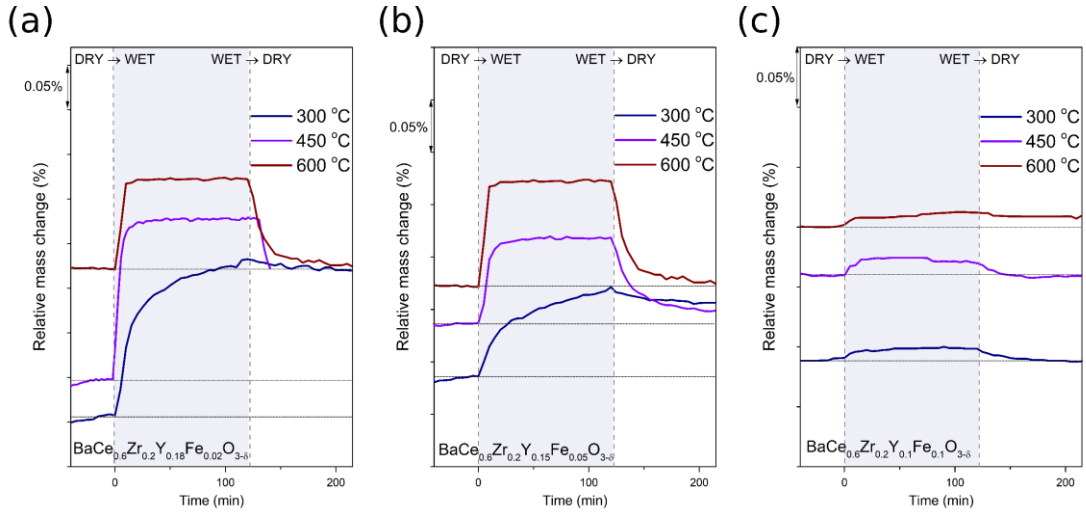

Fig. S2. Relative mass change of $BaCe_{0.6}Zr_{0.2}Y_{0.2-x}Fe_xO_{3-\delta}$ (x = 0.02, 0.05, 0.1) samples collected at 300, 450, and 600 °C during the atmosphere switches: from dry to wet and from wet to dry air.

3. Impedance data analysis

The Nyquist plots measured for $BaCe_{0.6}Zr_{0.2}Y_{0.2-x}Fe_xO_{3-\delta}$ (x = 0.02, 0.05, 0.1) samples with the fitted curves and equivalent circuits are presented in **Fig. S3**. Each plot corresponds to the measurement in dry and wet air atmosphere obtained at 300 and 800 °C.

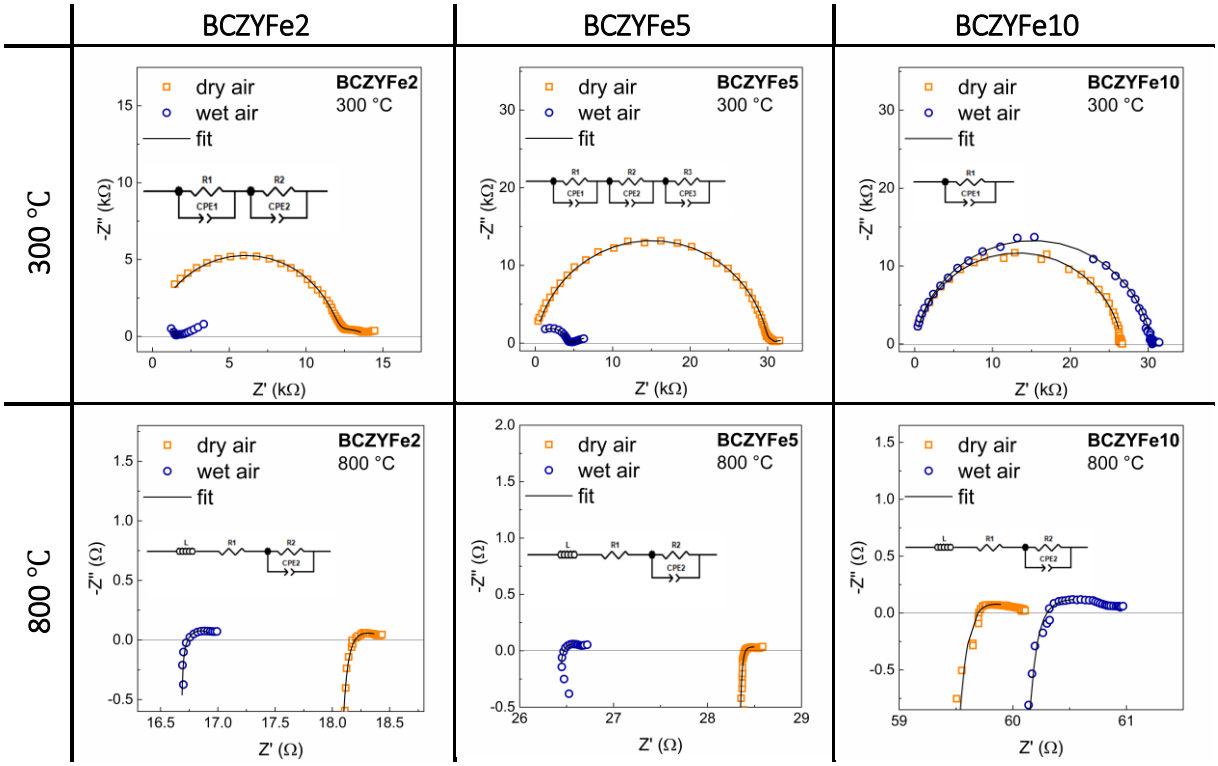

Fig. S3. XRD diffraction patterns with the corresponding fitting and differential curves for $BaCe_{0.6}Zr_{0.2}Y_{0.18}Fe_{0.02}O_{3-\delta}$ (BCZYFe2), $BaCe_{0.6}Zr_{0.2}Y_{0.15}Fe_{0.05}O_{3-\delta}$ (BCZYFe5), and $BaCe_{0.6}Zr_{0.2}Y_{0.1}Fe_{0.1}O_{3-\delta}$ (BCZYFe10), refined using cubic, orthorhombic and trigonal unit cells.

4. Additional Electrical Conductivity Relaxation (ECR) data and details about the fitting procedure

When oxygen or water is incorporated or released, the concentrations of charge carriers in the material changes due to the establishment of a new equilibrium. This affects the electrical conductivity of the material. The rate at which these changes occur varies depending on the chemical diffusion coefficient and chemical surface exchange coefficient of the incorporated species. The relationship between the concentration and the conductivity of the material can be mathematically represented by the equation (1).

$$\frac{C(t) - C(0)}{C(\infty) - C(0)} = \frac{\sigma(t) - \sigma(0)}{\sigma(\infty) - \sigma(0)}, \quad (1)$$

where $C(0)$ is the initial concentration of the considered species, $C(t)$ is the concentration at a given time, $C(\infty)$ is the equilibrium concentration of species, $\sigma(t)$ is the electrical conductivity of material at a given time, $\sigma(0)$ is the initial value of conductivity, and $\sigma(\infty)$ is the equilibrium conductivity.

The surface exchange and the bulk diffusion flux in the equilibrium state follow the equation (2):

$$-D_{chem}\frac{\partial C}{\partial x}\Big|_{x=\pm a} = k_{chem}[C(\infty) - C(\mathrm{t})], \tag{2}$$

where D_{chem} is a chemical diffusion coefficient, while k_{chem} is a chemical surface exchange coefficient. By solving this partial differential equation, the fitting function for the considered model can be obtained. In the case of samples investigated in this work, the 3D bar sample model was chosen, which can be described as a fitting function (3), in which D_{chem} and k_{chem} are the fitting parameters:

$$\frac{\sigma(t)-\sigma(0)}{\sigma(\infty)-\sigma(0)} = 1 - \sum_{m=1}^{\infty}\sum_{n=1}^{\infty}\sum_{p=1}^{\infty}\left\{\frac{2L_x^2\exp\left(-\frac{\alpha_m^2 D_{\mathrm{chem}}\,t}{x^2}\right)}{\alpha_m^2(\alpha_m^2+L_x^2+L_x)}\times\frac{2L_y^2\exp\left(-\frac{\beta_n^2 D_{\mathrm{chem}}\,t}{y^2}\right)}{\beta_n^2(\beta_n^2+L_y^2+L_y)}\times\frac{2L_z^2\exp\left(-\frac{\gamma_p^2 D_{\mathrm{chem}}\,t}{z^2}\right)}{\gamma_p^2(\gamma_p^2+L_z^2+L_z)}\right\}, \tag{3}$$

where L_x, L_y, and L_z represent a Biot numbers defined as

$$L_x = x\cdot\frac{k_{\mathrm{chem}}}{D_{\mathrm{chem}}}, L_y = y\cdot\frac{k_{\mathrm{chem}}}{D_{\mathrm{chem}}}, L_z = z\cdot\frac{k_{\mathrm{chem}}}{D_{\mathrm{chem}}}, \tag{4}$$

where x, y, and z are the half of the length, width, and thickness of sample, respectively. α_m, β_n, and γ_p are the positive roots of the equations

$$\alpha_m\tan(\alpha_m) = L_x, \beta_n\tan(\beta_n) = L_y, \gamma_p\tan(\gamma_p) = L_z. \tag{5}$$

For the purpose of this study, the L_z parameter (later denoted as L) was used to the determine the slower, limiting process during the relaxation measurements. If L reached values below 0.03, the limiting process was the surface exchange, whereas if it was above 30, the limiting process was the bulk diffusion. Therefore, if L was outside of this range, only one coefficient, corresponding to the limiting process, could be determined. If L value was within this range, both coefficients could be determined. The dimensions of samples studied during hydration/dehydration, as well as oxidation/reduction, by ECR method, the values of L parameter and the coefficients determined by fitting for each process and temperature are shown in **Table S2** and **S3**, respectively.

The ECR data was analyzed using NETL SOFC ECR Analysis software developed by the Solid Oxide Fuel Cell Research Team National Energy Technology Laboratory (NETL), U.S. Department of Energy (DOE).[1] Using this tool, it was possible to obtain chemical surface exchange coefficient and chemical diffusion coefficient of oxygen, hydrogen or water via the curve fitting approach. An assessment of electrical conductivity response was evaluated using nonlinear least squares method. The fitting ranges for D_{chem} and k_{chem} was set as 10^{-8} – 10^{4} cm^2/s and 10^{-6} – 10^{4} cm/s, respectively.

The exemplary ECR data with fitted curves for hydration and oxidation in the studied materials are presented in **Fig. S4** and **S5**, respectively. In the case of two-fold relaxation of water, the data was divided into H and O dominated regions and fitted separately as was shown in **Fig. S4a**.

[1] H. Abernathy, T. Yang, J. Liu and B. Na, 2021, DOI:10.18141/1762415, https://edx.netl.doe.gov/dataset/netl-electrical-conductivity-relaxation-ecr-analysis-tool.

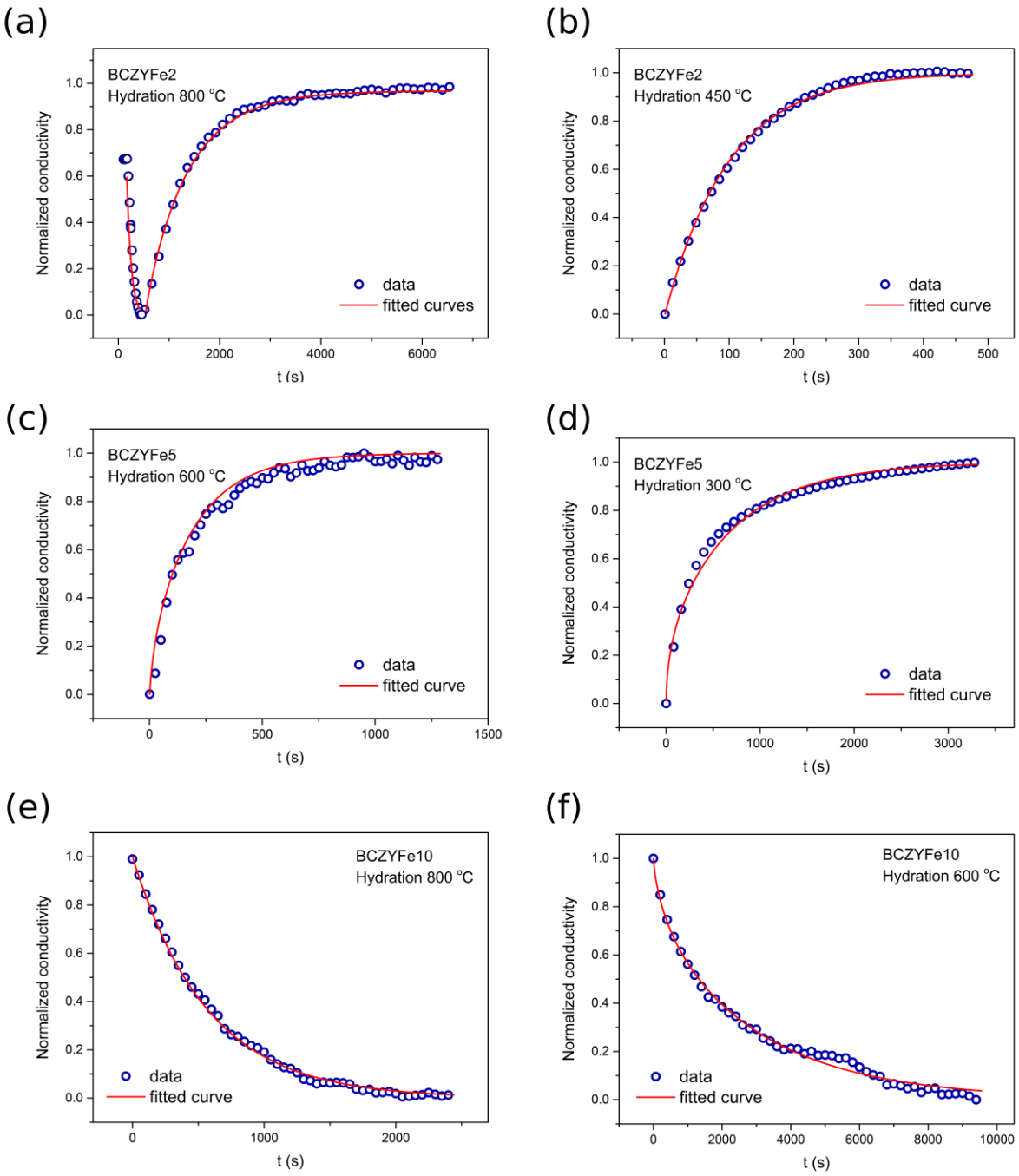

Fig. S4. The exemplary ECR data with the corresponding fitting curves for hydration of $BaCe_{0.6}Zr_{0.2}Y_{0.18}Fe_{0.02}O_{3-\delta}$ (a-b), $BaCe_{0.6}Zr_{0.2}Y_{0.15}Fe_{0.05}O_{3-\delta}$ (c-d), and $BaCe_{0.6}Zr_{0.2}Y_{0.1}Fe_{0.1}O_{3-\delta}$ (e-f).

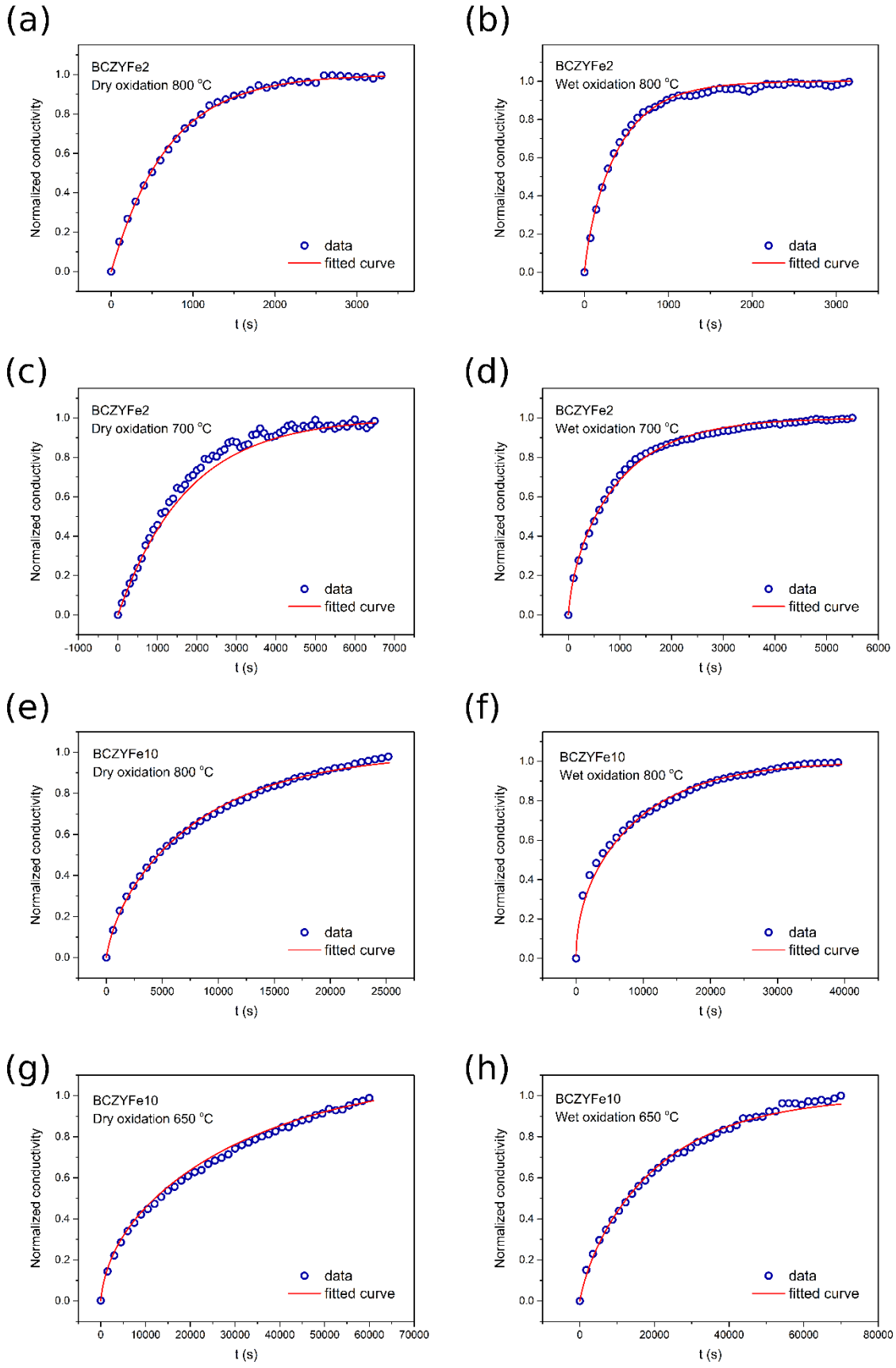

Fig. S5. The exemplary ECR data with the corresponding fitting curves for oxidation of $BaCe_{0.6}Zr_{0.2}Y_{0.18}Fe_{0.02}O_{3-\delta}$ (a-d), and $BaCe_{0.6}Zr_{0.2}Y_{0.1}Fe_{0.1}O_{3-\delta}$ (e-h) measured at dry and wet conditions.

Table S2. The dimensions of samples studied during hydration/dehydration by ECR method, the values of L parameter and the coefficients determined by fitting for each process and temperature.

Material	Dimensions of sample	Process	Temperature		L	Determined
BCZYFe2	14.9 mm × 8.1 mm × 1.75 mm	Hydration	850	H	$2.3 \cdot 10^{-5}$	k
				O	0.34	D and k
			800	H	$1.7 \cdot 10^{-5}$	k
				O	0.45	D and k
			750	H	$1.4 \cdot 10^{5}$	k
				O	0.86	D and k
			700	H	$1.7 \cdot 10^{-5}$	k
				O	1.4	D and k
			650	H	$1.1 \cdot 10^{-5}$	k
				O	1.8	D and k
			600	H	$2.7 \cdot 10^{-5}$	k
				O	2.3	D and k
			550	H	$1.9 \cdot 10^{-5}$	k
				O	4.6	D and k
			500	Single-fold	$1.9 \cdot 10^{-5}$	k
			450		$1.4 \cdot 10^{-4}$	k
			350		1.0	D and k
		Dehydration	850	H	$1.4 \cdot 10^{-5}$	k
				O	2.8	D and k
			800	H	$2.4 \cdot 10^{-5}$	k
				O	1.2	D and k
			750	H	$2.0 \cdot 10^{-5}$	k
				O	1.4	D and k
			700	H	$2.5 \cdot 10^{-5}$	k
				O	1.9	D and k
			650	H	$9.9 \cdot 10^{-5}$	k
				O	0.8	D and k
			600	H	$3.0 \cdot 10^{-5}$	k
				O	0.32	D and k
			550	H	$1.9 \cdot 10^{-5}$	k
				O	0.32	D and k
BCZYFe5	15.4 mm × 8.55 mm × 2.0 mm	Hydration	800	Single-fold	5.1	D and k
			750		5.2	D and k
			650		$7.4 \cdot 10^{7}$	D
			600		3.8	D and k
			550		7.7	D and k
			500		3.0	D and k
			450		3.3	D and k
			400		3.8	D and k
			350		2.0	D and k
			300		$1.2 \cdot 10^{7}$	D
		Dehydration	800		11.4	D and k
			750		22.2	D and k
			650		$7.6 \cdot 10^{6}$	D

			600		$8.4 \cdot 10^{6}$	D
			500		65	D
			450		80	D
			400		80	D and k
			350		$2.3 \cdot 10^{5}$	D
			300		$4.1 \cdot 10^{5}$	D
BCZYFe10	15.7 mm × 8.65 mm × 2.75 mm	Hydration	800		$2.4 \cdot 10^{5}$	k
			750		$6.8 \cdot 10^{-2}$	D and k
			700		$9.7 \cdot 10^{-2}$	D and k
			600		2.3	D and k
			550		2.5	D and k
			500		8.3	D and k
		Dehydration	800		0.42	k
			750		12	D and k
			700		$1.9 \cdot 10^{-5}$	k
			600		$3.1 \cdot 10^{-5}$	k
			550		$9.4 \cdot 10^{-5}$	k
			500		$4.0 \cdot 10^{-4}$	k

Table S3. The dimensions of samples studied during oxidation/reduction by ECR method, the values of L parameter and the coefficients determined by fitting for each process and temperature.

Material	Dimensions of sample	Process		Temperature	L	Determined
BCZYFe2	14.9 mm × 8.1 mm × 1.75 mm	Dry	Oxidation	800	$1.5 \cdot 10^{-5}$	k
				750	$3.5 \cdot 10^{-6}$	k
				700	$1.5 \cdot 10^{-5}$	k
				650	$8.1 \cdot 10^{-6}$	k
				600	$2.3 \cdot 10^{-6}$	k
			Reduction	800	12	D and k
				750	9.3	D and k
				700	12	D and k
				600	$1.1 \cdot 10^{6}$	D
		Wet	Oxidation	800	1.8	D and k
				750	0.27	k
				700	4.2	D and k
				650	2.5	D and k
			Reduction	800	2.7	D and k
				750	3.3	D and k
				700	3.5	D and k
				600	2.6	D and k
BCZYFe10	14.2 mm × 7.9 mm × 1.6 mm	Dry	Oxidation	800	15	D and k
				750	10	D and k
				700	16	D and k
				650	38	D
			Reduction	800	4.2	D and k

				750	6.2	D and k
				700	7.8	D and k
				650	$1.0 \cdot 10^3$	D
		Wet	Oxidation	800	4.5	D and k
				750	8.3	D and k
				700	9.3	D and k
				650	22	D and k
			Reduction	800	$1.1 \cdot 10^5$	D
				750	$3.1 \cdot 10^5$	D
				700	$8.3 \cdot 10^6$	D
				650	6.8	D and k